The American Journal of Pathology, Vol. 181, No. 2, August 2012

http://dx.doi.org/10.1016/j.ajpath.2012.04.004

Molecular Pathogenesis of Genetic and Inherited Diseases

AMPK Activation Stimulates Autophagy and Ameliorates Muscular Dystrophy in the *mdx* Mouse Diaphragm

Marion Pauly,* Frederic Daussin,† Yan Burelle,† Tong Li,‡ Richard Godin,† Jeremy Fauconnier,* Christelle Koechlin-Ramonatxo,§ Gerald Hugon,* Alain Lacampagne,* Marjorie Coisy-Quivy,* Feng Liang,‡ Sabah Hussain,‡ Stefan Matecki,* and Basil J. Petrof‡

From the Physiology and Experimental Medicine Heart-Muscle Unit, INSERM U1046, Montpellier 1 University, Montpellier, France; the Faculty of Pharmacy,† University of Montreal, Montreal, Quebec, Canada; the Meakins-Christie Laboratories and Respiratory Division,‡ McGill University Health Centre and Research Institute, Montreal, Quebec, Canada; and the Cellular Differentiation and Growth Unit,§ National Agronomic Research Institute-INRA-UMR A866, Montpellier, France*

Duchenne muscular dystrophy (DMD) is characterized by myofiber death from apoptosis or necrosis, leading in many patients to fatal respiratory muscle weakness. Among other pathological features, DMD muscles show severely deranged metabolic gene regulation and mitochondrial dysfunction. Defective mitochondria not only cause energetic deficiency, but also play roles in promoting myofiber atrophy and injury via opening of the mitochondrial permeability transition pore. Autophagy is a bulk degradative mechanism that serves to augment energy production and eliminate defective mitochondria (mitophagy). We hypothesized that pharmacological activation of AMP-activated protein kinase (AMPK), a master metabolic sensor in cells and on-switch for the autophagy-mitophagy pathway, would be beneficial in the *mdx* mouse model of DMD. Treatment of *mdx* mice for 4 weeks with an established AMPK agonist, AICAR (5-aminoimidazole-4-carboxamide-1-β-D-ribofuranoside), potently triggered autophagy in the *mdx* diaphragm without inducing muscle fiber atrophy. In AICAR-treated *mdx* mice, the exaggerated sensitivity of *mdx* diaphragm mitochondria to calcium-induced permeability transition pore opening was restored to normal levels. There were associated improvements in *mdx* diaphragm histopathology and in maximal force-generating capacity, which were not linked to increased mitochondrial biogenesis or up-regulated utrophin expression. These findings suggest that agonists of AMPK and other inducers of the autophagy-mitophagy pathway can help to promote the elimination of defective mitochondria and may thus serve as useful therapeutic agents in DMD. *(Am J Pathol 2012, 181:583–592; http://dx.doi.org/10.1016/j.ajpath.2012.04.004)*

Duchenne muscular dystrophy (DMD), the most common X-linked lethal disorder in humans, is caused by defects in the dystrophin gene.[1] Absence of dystrophin is associated with muscle fiber death involving both apoptosis and necrosis.[2] Because DMD affects the diaphragm and other respiratory muscles, many patients die of respiratory failure. Although the ideal treatment for DMD would be restoration of dystrophin expression to all muscles of the body, this is not currently feasible, and there is an urgent need for new therapies. The *mdx* mouse also lacks dystrophin, and is a commonly used animal model for studying the disease and its potential responsiveness to new treatments.[3]

Muscles lacking dystrophin exhibit multiple cellular defects, including abnormal fragility of the sarcolemma, increased oxidative stress, and elevated cytosolic calcium levels.[4] DMD muscles also show mitochondrial dysfunction and diminished expression of energy-producing metabolic genes.[5,6] Conversely, forced expression of the mitochondrial biogenesis factor peroxisome proliferator-activated receptor-γ coactivator 1-α (PGC-1α; official

Supported by grants from the Canadian Institutes of Health Research, the Health Research Fund of Quebec, the French National Health and Medical Research Institute, Researcher of the Future award from the Regional Council of Languedoc Roussillon, and the French Association Against Myopathies.

Accepted for publication April 5, 2012.

S.M. and B.J.P. contributed equally to this work.

Supplemental material for this article can be found at *http://ajp.amjpathol.org* or at *http://dx.doi.org/10.1016/j.ajpath.2012.04.004*.

Address reprint requests to Basil J. Petrof, M.D., McGill University Health Centre, Royal Victoria Hospital Site, Respiratory Division, Room L4.11, 687 Pine Ave. West, Montreal, QC, H3A 1A1, Canada. E-mail: basil.petrof@mcgill.ca.

symbol, PPARGC-1-α) ameliorates dystrophic pathology in *mdx* mice.[7] AMP-activated protein kinase (AMPK), a major sensor of cellular energy status, switches on mechanisms favoring ATP generation under conditions of energetic deficiency.[8] Thus, AMPK can stimulate mitochondrial biogenesis through the PGC-1-α pathway, as well as through catabolic pathways that fuel energy production. Chief among these catabolic mechanisms is the lysosomally mediated process of macroautophagy (henceforth referred to simply as autophagy), which targets cellular constituents that are too large to be removed by other degradative pathways.[9,10]

In addition to its energy-producing function, autophagy plays a critical role in cellular quality control by preferentially eliminating proteins and organelles that are nonessential or dysfunctional, including defective mitochondria.[9,10] Recent work has linked defects in autophagic removal of mitochondria (mitophagy) to Parkinson's disease and other neurodegenerative diseases, as well as to muscular dystrophy associated with collagen VI deficiency.[11,12] Impaired mitophagy permits the accumulation of damaged mitochondria, which not only perform poorly in their energy-generating role but also have a greater propensity to undergo opening of the mitochondrial membrane permeability transition pore (PTP) complex.[12,13] This leads to mitochondrial swelling, collapse of the mitochondrial membrane potential, and release of proapoptotic factors, which have been implicated not only in cell death but also in muscle fiber atrophy and injury.[14,15]

In the present study, we postulated that therapeutic activation of AMPK might stimulate autophagic removal of defective mitochondria in *mdx* mice, thereby leading to beneficial effects on mitochondrial PTP opening, as well as on the overall muscular dystrophy phenotype. To test this hypothesis, we treated *mdx* mice with AICAR (5-aminoimidazole-4-carboxamide-1-β-D-ribofuranoside), an established pharmacological activator of AMPK[16] that has been shown to promote mitophagy.[17] We focused the present study on the *mdx* mouse diaphragm, because this model closely mimics human DMD with respect to both fiber loss and weakness.[3] Here, we show that chronic AICAR treatment effectively stimulates autophagy, increases the ability of muscle fiber mitochondria to resist PTP opening, and ameliorates histological features of muscular dystrophy, as well as muscle strength in the *mdx* diaphragm. These results support the concept that promoting the autophagic removal of defective mitochondria via AMPK stimulation could be a useful therapeutic strategy in DMD patients.

Materials and Methods

Animals and Cell Culture

Six-week-old male *mdx* mice (Jackson Laboratories, Bar Harbour, ME) received intraperitoneal injections of AICAR (Toronto Research Chemicals, Toronto, ON, Canada) at a daily dose of 500 mg/kg body weight (5 consecutive days per week) for 4 weeks.[16] Untreated littermate *mdx* mice were injected in the same manner with vehicle (0.9% NaCl); wild-type (WT) (C57BL6) mice (Janvier SAS, Le Genest Saint Isle, France) did not receive any treatment. Primary myotube cultures from *mdx* mice were derived from single living myofibers, as described previously.[18] The investigation complied with the Guide for the Care and Use of Laboratory Animals (2011 edition).

Immunoblotting and Gene Expression Analysis

Immunoblotting was performed by standard methods using antibodies against phospho-AMPKα (Thr^{172}), total AMPKα, phospho-ACC (Ser^{79}), total ACC, LC3, Beclin-1, phospho-mTOR (Ser^{2448}), total mTOR, phospho-raptor (Ser^{792}), total raptor, phospho-p70S6K (Thr^{389}), and total p70S6K from Cell Signaling Technology (Danvers, MA); Ulk1, Bnip3, β-actin, and tubulin from Sigma-Aldrich (St. Louis, MO); mitochondrial respiratory complex subunits (I-20 kDa; II-30 kDa; III-47 kDa; V-53 kDa) from MitoSciences (Eugene, OR); GAPDH from Abcam (Cambridge, UK); and utrophin, with a polyclonal antibody previously characterized by our laboratory.[19] Analysis and quantification (normalized in all cases to indicated loading control proteins) were performed with ImageJ software version 1.43u (NIH, Bethesda, MD). Real-time PCR to quantify mRNA levels was performed using Fast SYBR Green (Applied Biosystems) and the cycle threshold method.

Immunohistochemistry and Morphometry

Transverse cryosections stained by H&E were used for determination of fiber size and the percentage of centrally nucleated fibers, with a minimum of five cross sections per muscle, each containing an average of 100 fibers.[20] For determination of fiber types, adjacent sections were immunostained with anti-slow type 1 (M-8421; Sigma-Aldrich) and anti-fast type 2a (mAb SC-71; Santa Cruz Biotechnology, Santa Cruz, CA) antibodies. Electron microscopy was performed on muscle tissues as described previously.[20]

Mitochondrial Enzyme and Respiration Assays

Mitochondrial enzyme and respiration assays were performed as described previously.[21] Briefly, activities of citrate synthase and cytochrome c oxidase (COX) were determined spectrophotometrically using standard coupled enzyme assays. Mitochondrial respiration was analyzed in an oximeter equipped with a Clarke type of electrode. The chamber was filled with the following solution: 2.77 mmol/L CaK_2-EGTA, 7.23 mmol/L K_2-EGTA (100 nmol/L free Ca^{2+}), 6.56 mmol/L $MgCl_2$ (1 mmol/L free Mg^{2+}), 20 mmol/L taurine, 0.5 mmol/L dithiothreitol, 50 mmol/L potassium-methane sulfonate (160 mmol/L ionic strength), and 20 mmol/L imidazole (pH 7.1). After the baseline oxygen content in the chamber had been recorded, one bundle of 1 to 2 mg dry weight of saponin-permeabilized myofibers was placed into the chamber. Readings were taken of the rate of O_2 consumption per unit time, first basally in the presence of glutamate plus malate (10:5, mmol/L), and then after the addition of ADP (2 mmol/L). Respiration rates were measured at 23°C under

continuous stirring. At the end of each test, fibers were carefully removed from the oxygraphic cell, blotted, and dried for determination of fiber weight. Rates of O_2 consumption were expressed in nmol O_2/minute per per milligram dry weight.

Mitochondrial H_2O_2 Release and Scavenging

Mitochondrial H_2O_2 dynamics were measured in dissected fiber bundles with the fluorescent probe Amplex Red (20 μmol/L; Invitrogen), as described previously.[21] After saponin permeabilization, the fibers were rinsed three times in the following buffer maintained at 4°C and at pH 7.3: 110 mmol/L K-2-(*N*-morpholino)ethanesulfonic acid, 35 mmol/L KCl, 1 mmol/L EGTA, 5 mmol/L K_2HPO_4, 3 mmol/L $MgCl_2 \cdot 6H_2O$, and 0.5 mg/mL BSA. Fiber bundles (0.3 to 1.0 mg dry weight) were then incubated in a quartz microcuvette with continuous magnetic stirring in the same buffer supplemented with 1.2 U/mL horseradish peroxidase at 37°C. Baseline fluorescence readings were taken in the absence of any exogenous respiratory substrates. The following additions were then made sequentially: 5 mmol/L succinate, 10 mmol/L ADP, and 8 μmol/L antimycin A. To determine H_2O_2 scavenging capacity, permeabilized fiber bundles were placed in the above buffer containing additionally 50 μmol/L pyruvate and 20 μmol/L malate in a thermally controlled chamber set at 37°C with continuous stirring. An aliquot of the buffer was removed immediately after adding 40 μmol/L of H_2O_2 and subsequently at 20, 40, and 60 seconds. H_2O_2 content in aliquots was determined immediately on a fluorescence plate reader in a buffer containing 10 μmol/L of Amplex Red and 0.5 U/mL horseradish peroxidase. The rate of H_2O_2 scavenging by mitochondria was determined as the difference between fluorescence levels obtained at time $t = 0$. Rates of H_2O_2 production and scavenging were calculated from standard curves established under corresponding experimental conditions. All measurements were performed at least in duplicate, and results were expressed in nmol H_2O_2 scavenged per minute per milligram dry weight.

Mitochondrial PTP Function

The PTP opening time and calcium retention capacity were determined by fluorimetrically monitoring changes in extramitochondrial calcium concentration, using the probe Calcium Green-5N (Invitrogen-Life Technologies, Carlsbad, CA), after exposing fibers to a single pulse of external calcium.[21,22] Ghost fibers were first prepared by incubating saponin-permeabilized bundles in a high-KCl medium, to extract myosin. The ghost fibers were then incubated at 23°C in a quartz microcuvette under continuous stirring in the following buffer: 250 mmol/L sucrose, 10 mmol/L 3-(*N*-morpholino)propanesulfonic acid, 0.005 mmol/L EGTA, and 10 mmol/L propidium iodide-Tris (pH 7.3), supplemented with glutamate plus malate (5:2.5, mmol/L) and 0.5 nmol/L oligomycin. After adding 20 nmol Ca^{2+} to the buffer, PTP opening time was taken as the time lapse between addition of the Ca^{2+} pulse and the time at which Ca^{2+} release was first noted to occur. Calcium retention capacity was defined as the total amount of Ca^{2+} accumulated by mitochondria before Ca^{2+} release caused by PTP opening, expressed per milligram wet fiber weight. Ca^{2+} concentration in the cuvette was calculated from a standard curve relating [Ca^{2+}] to the fluorescence of Calcium Green-5N.

Measurement of Skeletal Muscle Contractile Properties

Diaphragm strips were electrically stimulated to determine intrinsic contractile properties, as described previously.[23] After euthanasia, the diaphragm was surgically excised and immediately transferred to chilled Krebs solution perfused with 95% O_2:5% CO_2 (pH 7.4). From the central tendon to the rib, a 2-mm-wide muscle strip was dissected free and mounted between two electrodes within a jacketed tissue bath chamber filled with continuously perfused Krebs solution warmed to 25°C. A 4-0 silk thread was used to secure the central tendon to an isometric force transducer. After a 15-minute thermoequilibration period, muscle length was gradually adjusted to optimal length (L_o, the length at which maximal twitch force is obtained). The force-frequency relationship was determined by sequential supramaximal stimulation for 1 second over a range of stimulation frequencies (from 10 to 120 Hz), with 2 minutes between each stimulation train. Fatigue resistance was assessed by measuring the rate of loss of muscle force during repetitive stimulation at 30 Hz over a 10-minute period. At the end of the experiment, L_o was directly measured with a microcaliper and the muscle was blotted dry and weighed. Specific force (force/cross-sectional area) was calculated and expressed in newtons per square centimeter, assuming a muscle density of 1.056 g/cm^3.

Statistical Analysis

Data are expressed as means ± SEM. Statistical significance was defined as $P < 0.05$, using Student's unpaired *t*-test or analysis of variance (one- or two-way), followed by a Bonferroni selected-comparison test.

Results

Premature Mitochondrial PTP Opening and Energetic Deficiency in Dystrophic Muscle

Dystrophic diaphragms contained numerous fibers with morphologically abnormal mitochondria, characterized by a rounded swollen appearance and grossly disrupted internal structure (Figure 1A). To examine the ability to resist PTP opening, which is a critically important aspect of mitochondrial function, permeabilized fibers were exposed to an external calcium load. The mitochondria of *mdx* diaphragms underwent significantly earlier PTP opening than observed in WT controls (Figure 1B). In keeping with these morphological and functional signs of defective mitochondria,

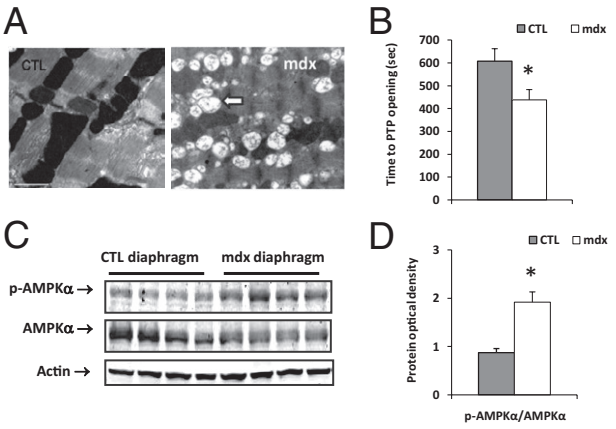

Figure 1. Defective mitochondria and premature PTP opening in *mdx* diaphragm fibers. **A:** Electron micrographs demonstrating differences in mitochondrial morphology between normal WT (CTL) and *mdx* diaphragms. Note numerous swollen mitochondria with abnormal cristae (**arrow**) in the *mdx* group. Scale bar = 1 μ. **B:** Time to mitochondrial permeability transition pore (PTP) opening after calcium challenge in *mdx* versus WT diaphragm fibers. **C:** Representative immunoblots showing baseline levels of phosphorylated and total forms of AMPK in WT and *mdx* diaphragms. **D:** Optical density quantification of p-AMPKα/total AMPKα protein levels (arbitrary units normalized to actin). Data are expressed as means ± SEM. $^{*}P < 0.05$. $n = 7$ to 9 per group (**B** and **D**).

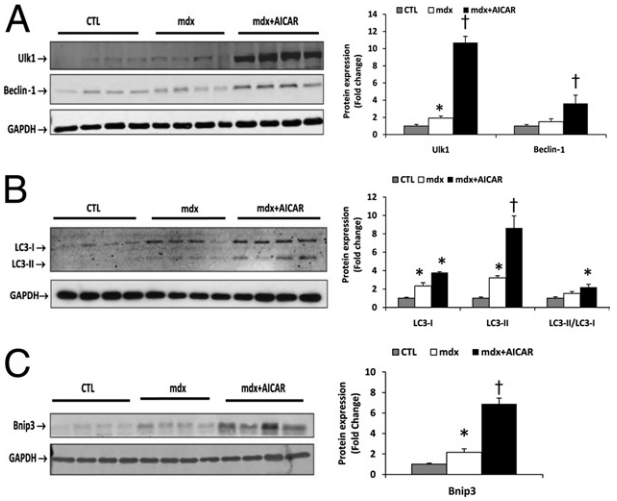

Figure 3. AICAR activates the autophagy pathway in *mdx* diaphragms. Representative immunoblots showing protein expression levels of Ulk1 and Beclin-1 (**A**), LC3-I and LC3-II (**B**), and Bnip3 (**C**) within the diaphragms of WT mice (CTL), untreated *mdx* mice, and AICAR-treated *mdx* mice. All quantifications of autophagy pathway proteins are normalized to GAPDH in terms of fold-change relative to WT mice. Data are expressed as means ± SEM. $n = 4$ to 6. $^{*}P < 0.05$ versus wild type; $^{\dagger}P < 0.05$ versus *mdx*.

baseline levels of AMPK activation (phosphorylation) were also higher in *mdx* than in WT diaphragms (Figure 1, C and D), which is consistent with cellular sensing of relative energetic deficiency within dystrophic myofibers.

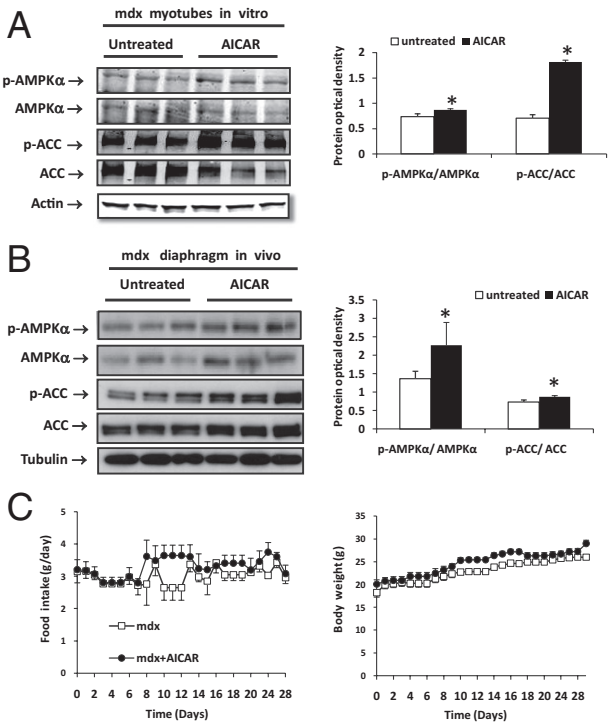

Figure 2. AICAR promotes AMPK activation in dystrophic muscles *in vitro* and *in vivo*. **A** and **B:** Phosphorylated and total forms of AMPK and acetyl CoA carboxylase (ACC) in primary myotube cultures derived from *mdx* mice, either without or with AICAR treatment (1 mmol/L for 24 hours) (**A**) and in dystrophic *mdx* diaphragms *in vivo*, either without or with AICAR treatment (500 mg/kg/day intraperitoneally for 48 hours) (**B**). Optical density quantification is in arbitrary units, normalized to actin or tubulin. **C:** Food intake and body weight of *mdx* mice during 4 weeks of receiving AICAR treatment or vehicle alone. Data are expressed as means ± SEM. $n = 8$ per group. $^{*}P < 0.05$.

AICAR Treatment Activates AMPK and ACC in Dystrophic Muscle

To determine whether short-term AICAR treatment could further boost AMPK activation in dystrophic muscle, we first examined AICAR effects on phosphorylation of AMPK and its downstream target, ACC (acetyl CoA carboxylase) in primary *mdx* myotubes. AICAR induced phosphorylation of the α-subunit of AMPK and to an even greater extent ACC *in vitro* (Figure 2A). As expected, AICAR also induced increased activation of AMPK *in vivo*, such that increased phosphorylation levels of both AMPK and ACC were observed in the diaphragms of *mdx* mice within 48 hours after AICAR treatment was initiated (Figure 2B). Food intake did not differ significantly between the untreated and AICAR-treated *mdx* groups for the study period as a whole, from 6 to 10 weeks of age, although it was briefly increased in the AICAR-treated group from days 10 to 12. Similarly, there were no significant differences in body weight between the untreated and AICAR-treated *mdx* mice over the total treatment period (Figure 2C).

AICAR Treatment Induces Autophagy and Improves Mitochondrial PTP Function

After 4 weeks of AICAR treatment *in vivo*, there was a major up-regulation of multiple components of the autophagy program in *mdx* diaphragms. This was reflected by increases in the mammalian Atg1 homolog, Ulk1 (an autophagy-initiating kinase that is directly activated by AMPK), as well as in Beclin-1, a component of the class III phosphoinositide 3-kinase complex involved in the initiation of autophago-

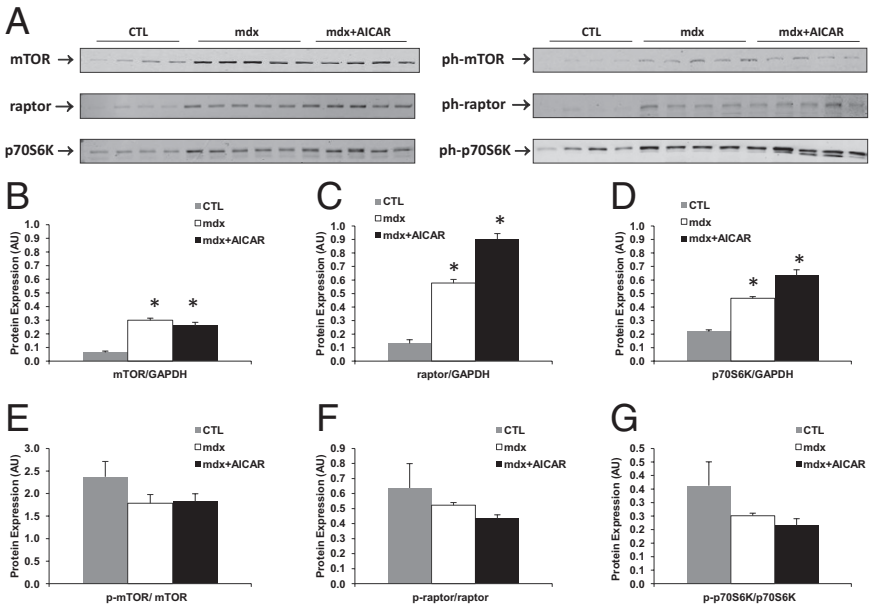

Figure 4. AICAR treatment does not alter mTORC1 activation in *mdx* diaphragms. Representative immunoblots (**A**) and quantification of protein levels for the total forms of mTOR (**B**), raptor (**C**), and p70S6K (**D**), as well as their relative phosphorylation levels (**E–G**), within the diaphragms of WT mice (CTL), untreated *mdx* mice, and AICAR-treated *mdx* mice. Optical density quantification is in arbitrary units, normalized to GAPDH in all cases. Data are expressed as means ± SEM. $n = 4$ or 5. $^*P < 0.05$ versus wild type.

somes (Figure 3A). In addition, the AICAR-treated group demonstrated higher levels of LC3-II, the lipidated form of LC3 that is generated during the process of autophagosome formation, and in the ratio of LC3-II to LC3-I (Figure 3B). Bnip3, a mitochondria-associated protein that plays a crucial role in the autophagic removal mitochondria in skeletal muscle was also found to be significantly up-regulated in the diaphragms of AICAR-treated *mdx* mice (Figure 3C). The levels of Ulk1, LC3, and Bnip3 were all mildly increased above WT levels in untreated *mdx* mice, suggesting that a degree of autophagic induction occurs basally in *mdx* diaphragms, most likely as an adaptive response to the dystrophic disease process itself.

The mammalian target of rapamycin (mTOR) exists within two functional complexes, mTORC1 and mTORC2, with the former being directly regulated by cellular energy status.[24] To determine whether the stimulation of autophagy by AICAR was associated with mTORC1 modulation in *mdx* diaphragms, we measured total and phosphorylated protein levels of key mTORC1 members, mTOR and raptor, as well as p70S6K, the downstream target of activated mTOR (Figure 4A). Levels of total mTOR, raptor, and p70S6K were all increased above WT levels in the two groups of *mdx* mice (Figure 4, B–D). However, the phosphorylated forms of these proteins increased in a proportionate fashion, and the ratios of phosphorylated to total forms of these proteins did not differ significantly between the untreated and AICAR-treated *mdx* mice (Figure 4, E–G).

Given that autophagy is an important mechanism for eliminating damaged mitochondria, we next sought to determine whether AICAR treatment led to improved mitochondrial PTP function. In AICAR-treated *mdx* mice, electron microscopy suggested qualitative improvements in mitochondrial morphology (Figure 5A). Importantly, the abnormal susceptibility to PTP opening observed in *mdx* diaphragm fibers was reversed in AICAR-treated *mdx* mice (Figure 5B). There were no statistically significant differences in global calcium retention capacity of mitochondria between WT, *mdx*, and *mdx*+AICAR groups (1.17 ± 0.18, 1.37 ± 0.27, and 1.69 ± 0.28 nmol Ca^{2+} per milligram, respectively). Thus, the major findings are that the autophagic process in dystrophic muscles is greatly boosted by chronic administration of AICAR, and that this is associated with a significantly greater ability of mitochondria to resist calcium-induced membrane permeabilization.

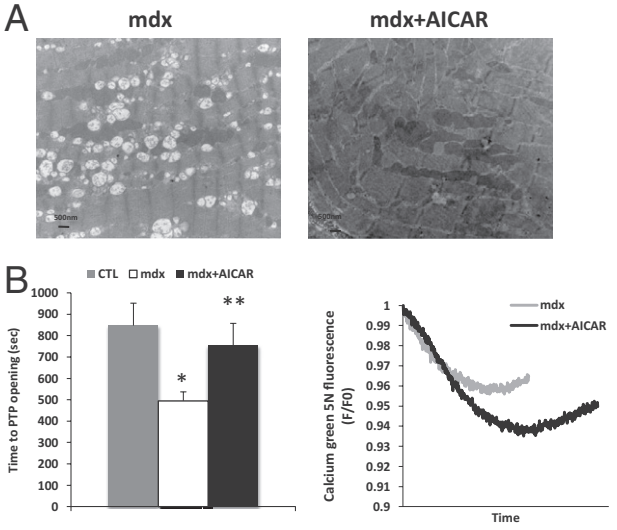

Figure 5. AICAR improves mitochondrial PTP function in *mdx* diaphragm fibers. **A:** Electron microscopic images of mitochondria in *mdx* and *mdx*+AICAR diaphragms. **B:** Effects of AICAR treatment on PTP opening time in *mdx* diaphragms (**left**) in WT mice (CTL), untreated *mdx* mice, and AICAR-treated *mdx* mice, as well as a representative tracing of mitochondrial calcium uptake and release within permeabilized fibers after calcium challenge (**right**). Data are expressed as means ± SEM. $n = 7$ to 10 per group. $^*P < 0.05$ versus WT; $^{**}P < 0.05$ versus *mdx*. Scale bar = 500 nm.

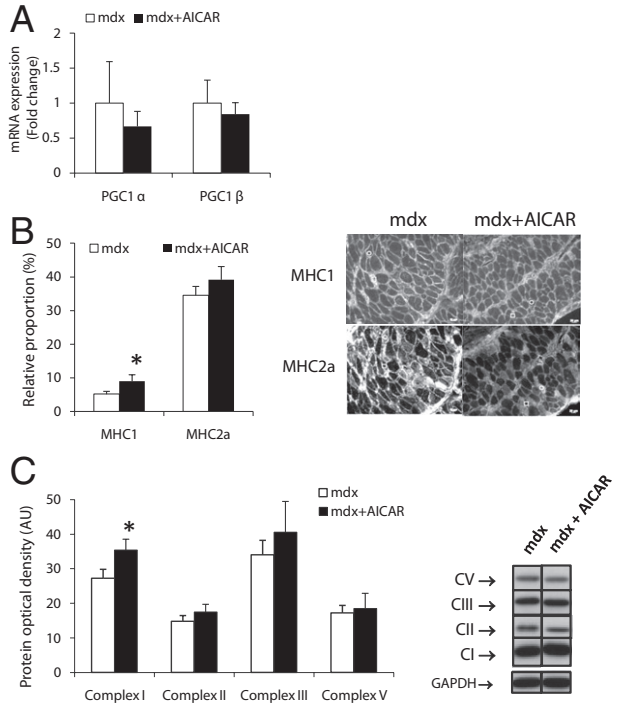

Figure 6. AICAR effects on oxidative fiber types and mitochondrial complexes. **A:** mRNA levels of transcription factor genes associated with mitochondrial biogenesis, reported in terms of fold change relative to untreated *mdx* diaphragms. Scale bars: 20 μ. **B:** Comparison of relative proportion of fiber types in the diaphragms of untreated *mdx* and AICAR-treated *mdx* mice; micrographs show serial transverse muscle sections (with same fibers indicated by small circle and square) immunostained for type 1 or type 2a myosin heavy chain (MHC) expression. **C:** Quantification of respiratory chain complexes in untreated *mdx* and AICAR-treated *mdx* mice, with immunoblotting for the same complexes (CI, CII, CIII, and CV). Protein and mRNA levels are normalized to housekeeping GAPDH. Data are expressed as means ± SEM. $n = 6$ to 10 per group. $^*P < 0.05$.

Lack of AICAR Effects on Mitochondrial Biogenesis and Oxidative Functions

In addition to autophagy, improved mitochondrial PTP function after AICAR treatment could be the result of enhanced mitochondrial biogenesis and its accompanying antioxidant effects. Therefore, we evaluated whether AICAR reprogrammed the *mdx* diaphragm to a more oxidative phenotype. At 4 weeks after initiation of AICAR treatment, the mRNA levels for PGC-1-α and PGC-1-β, two transcription factors typically associated with activation of the mitochondrial biogenesis program, were unchanged compared with untreated mice (Figure 6A). In AICAR-treated *mdx* mice, there was a small increase in type 1 (slow oxidative) fibers, but without any alteration in type 2a (fast oxidative) fibers in the diaphragm (Figure 6B). Immunoblotting revealed increased mitochondrial complex I protein expression without changes in complexes II, III, or V (Figure 6C). Levels of the dystrophin homolog protein utrophin, which is up-regulated in *mdx* muscles and typically is expressed at higher levels in oxidative fibers,[25] were similarly unaltered by AICAR treatment in *mdx* diaphragms (see Supplemental Figure S1 at *http://ajp.amjpathol.org*).

The above findings suggesting minimal effects of chronic AICAR administration on the overall oxidative capacity of *mdx* diaphragms were further examined at a functional level. Enzymatic activity levels of both mitochondrial citrate synthase and cytochrome c oxidase (COX) in the diaphragm were unaffected by AICAR administration (Figure 7A). In addition, basal (V_0) and maximal (V_{max}) rates of oxygen consumption by *mdx* diaphragm fibers were unchanged (Figure 7B). Antioxidant function was determined by measuring H_2O_2 fluxes from permeabilized fibers using Amplex Red. Neither the H_2O_2 scavenging capacity (Figure 7C) nor H_2O_2 release under conditions of altered substrate supply or of inhibition of the mitochondrial electron transport chain (Figure 7D) was affected by AICAR treatment. Overall, these findings indicate that improvements in mitochondrial PTP function in the *mdx* diaphragm after AICAR treatment were not linked to the development of a substantially more oxidative fiber type.

AICAR Treatment Improves Dystrophic Muscle Structure and Contractile Function

To establish whether autophagic induction and improved mitochondrial PTP function were associated with any amelioration of the muscular dystrophy phe-

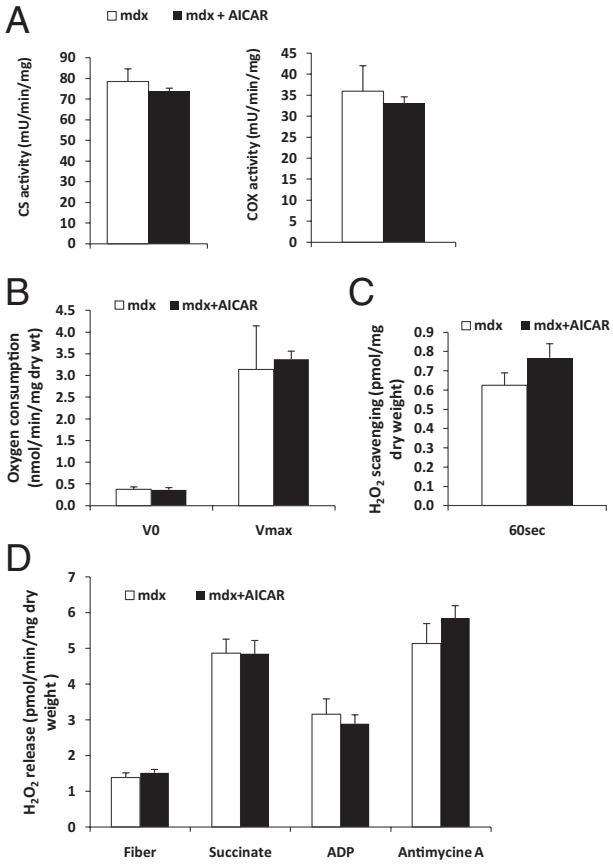

Figure 7. Lack of AICAR treatment effects on oxidative function. **A:** Citrate synthase (CS) and cytochrome c oxidase (COX) activity levels. **B:** Rate of O_2 consumption per unit of time, basally in the presence of glutamate plus malate (V_0) and after the addition of ADP (V_{max}). **C:** H_2O_2 scavenging as indicated by levels at 60 seconds after addition of H_2O_2 (40 μmol/L) to permeabilized fibers. **D:** Net rate of mitochondrial H_2O_2 release from permeabilized diaphragm fibers under basal conditions (Fiber) and after the addition of succinate, ADP, or antimycin A. Data are expressed as means ± SEM. $n = 8$ to 10 per group.

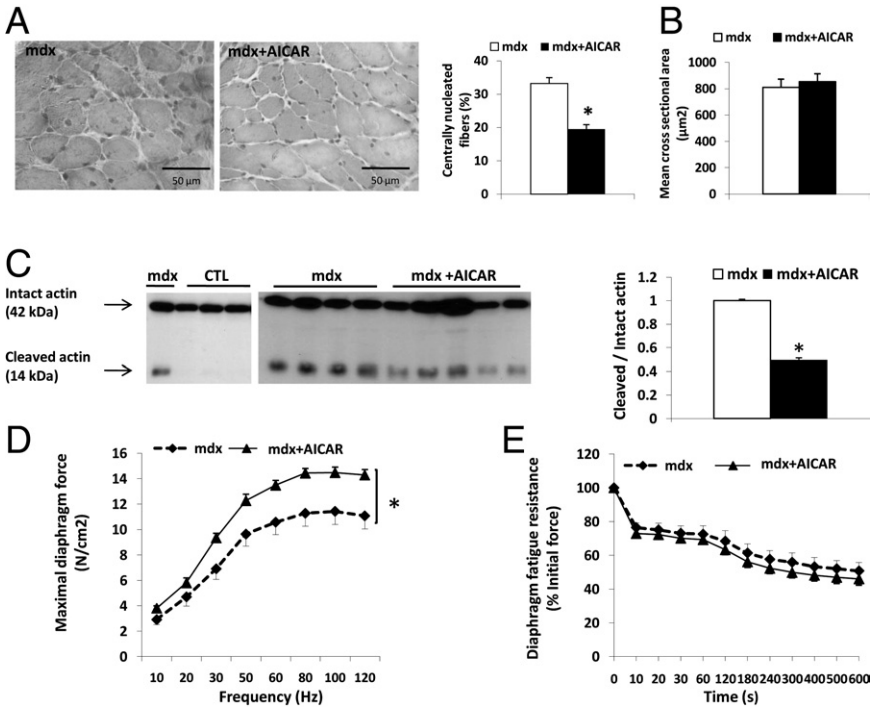

Figure 8. Beneficial effects of AICAR-treated relative to untreated *mdx* diaphragms. **A:** Representative H&E staining and percentages of diaphragm myofibers with centrally located nuclei. **B:** Mean cross-sectional area of diaphragm myofibers. **C:** Immunoblotting for actin, as well as the ratio between cleaved (14 kDa) and full-length forms of the protein, relative to untreated *mdx* diaphragms. **D:** Maximal force-generating capacity of the diaphragm *ex vivo* at different frequencies of electrical stimulation. **E:** Fatigue resistance of the diaphragm during repetitive electrical stimulation. Data are expressed as means ± SEM. $n = 8$ per group (**B**, **D**, and **E**); $n = 5$ per group (**C**). $^*P < 0.05$. CTL, WT control. Scale bar = 50 μm.

notype in the diaphragm, we first performed histological analysis of untreated versus AICAR-treated *mdx* mice. Muscle fibers with centrally located nuclei are a hallmark of previously regenerated muscle, and their relative proportion is therefore considered reflective of prior episodes of muscle fiber necrosis in *mdx* mice.[26,27] In AICAR-treated *mdx* mice, the diaphragm showed a reduction in the percentage of centrally nucleated fibers (Figure 8A), consistent with a mitigation of prior necrosis. Moreover, despite the increased level of autophagy in the AICAR group, the mean cross-sectional area of individual diaphragmatic muscle fibers was unaffected (Figure 8B), indicating that chronic AICAR administration did not induce fiber atrophy. In keeping with the lack of atrophy, AICAR treatment also partially eliminated the pathological presence in *mdx* diaphragms of a 14-kDa actin cleavage product that has previously been shown to be a reliable biomarker of skeletal muscle wasting (Figure 8C).[28,29]

Finally, to determine effects on contractile function, we compared the force-generating capacities of untreated and AICAR-treated *mdx* diaphragm muscle strips electrically stimulated *ex vivo*. AICAR-treated *mdx* mice demonstrated significantly greater diaphragmatic force production over a broad range of stimulation frequencies (30 to 120 Hz) (Figure 8D). In this regard, the maximal tetanic force production by the diaphragm increased by a mean of 21% ($P < 0.005$) in AICAR-treated *mdx* mice. On the other hand, endurance properties (fatigue resistance) of the diaphragm were unaffected by AICAR treatment (Figure 8E), which is consistent with its lack of physiologically important effects on oxidative capacity.

Discussion

Skeletal muscles lacking dystrophin have a reduced capacity for oxidative phosphorylation, and the diminished energy-producing potential of dystrophic muscle has been characterized as a metabolic crisis.[5,6] The metabolic sensor AMPK plays a key role in orchestrating the adaptive changes, including autophagy, that permit the survival of cells faced with energetic stress.[8] Autophagy not only supplies substrates for cellular energy production, but also provides a mechanism for more efficient use of these substrates via the removal of dysfunctional mitochondria.[11,17] In the present study, we postulated that pharmacological activation of AMPK would promote this normal adaptive response and thus have beneficial effects on the physiological function of the *mdx* diaphragm. The diaphragm is the primary muscle of respiration, and its involvement by the disease in DMD is responsible for the majority of patient deaths. In addition, in the *mdx* mouse model the diaphragm is the most severely affected muscle and bears the greatest resemblance to the human DMD phenotype.[3]

Our investigation revealed several new findings. First, *mdx* mice show evidence for increased autophagy and augmented AMPK activation at baseline, which suggests an adaptive response to the presence of mitochondrial damage and energetic stress. Second, AICAR treatment led to a further major increase in activation of the autophagy pathway, as indicated by the characteristic biochemical changes of increased LC3-II content and upregulation of other prototypical autophagy-associated proteins.[9] Third, in comparison with untreated *mdx* mice, the AICAR-treated group showed an improved ability to maintain mitochondrial integrity, as indicated by a greater

resistance to PTP opening in the face of calcium overload. Fourth, and most importantly, AICAR treatment of *mdx* mice for 4 weeks led to significant improvements in both muscle structure and maximum force-generating capacity of the *mdx* diaphragm.

Autophagy has been linked to situations associated with an inhibition of mTORC1 activation, such as nutrient deprivation, hypoxia, endoplasmic reticulum stress, and infections.[9,10] However, autophagy can also be triggered without the direct participation of mTORC1. For example, Beclin-1 can be activated by the stress-responsive c-Jun amino-terminal kinase 1 (JNK1) and death-associated protein kinase (DAPK) in an mTOR-independent fashion.[30,31] Acute AMPK stimulation by AICAR has been shown to initiate autophagy through complex interrelated mechanisms involving activation of the tuberous sclerosis complex (TSC), inhibition of mTORC1, phosphorylation of raptor, and activation of Ulk1.[17,32,33] In the present study, chronic AICAR administration induced autophagy in *mdx* diaphragms, but this was not associated with evidence of mTORC1 inhibition. Thus, the phosphorylation status (ie, the phosphorylated fraction) was unaltered not only for mTOR, but also for its partner raptor and the downstream target p70S6K. We therefore speculate that AICAR-induced autophagy in our model may have occurred, at least in part, through an mTOR-independent mechanism. This could potentially involve the direct phosphorylation of Ulk1 by AMPK, as recently described by different groups of investigators.[17,32,33] Rapamycin therapy from 6 to 12 weeks of age in *mdx* mice was recently reported to improve dystrophic histopathology in the diaphragm and tibialis anterior muscles, but once again with no consistent relationship to mTOR phosphorylation status.[34]

Whether autophagy is beneficial or harmful for skeletal muscle is dependent on its magnitude and on the specific context in which it occurs. Both excessive and inadequate autophagy can lead to muscle fiber atrophy in various disease states.[35] AICAR administration did not induce muscle fiber atrophy in the present study, suggesting that the autophagic process induced by AICAR was tightly regulated in its magnitude and/or was selective for dysfunctional cellular components. Although it may seem somewhat counterintuitive, previous work has shown that autophagy is actually required to maintain normal muscle mass.[36] Thus, autophagy-deficient knockout mice exhibit fiber atrophy, as well as increases in abnormal mitochondria and apoptosis.[36,37] Along these same lines, muscular dystrophies linked to collagen VI deficiency have an autophagy defect leading to the accumulation of dysfunctional mitochondria and exaggerated apoptosis, which can be significantly ameliorated by the forced activation of autophagy.[12] At an appropriate level, therefore, autophagy and, more particularly, mitophagy appear to be important homeostatic mechanisms in skeletal muscle that are necessary for ensuring mitochondrial quality control through the removal of damaged or dysfunctional mitochondria, as well as for the maintenance of normal muscle mass.

In addition to their primordial role in cellular energy production, mitochondria act as a calcium sink that can buffer and locally modulate cytosolic calcium levels.[38] When this mechanism is overwhelmed, however, mitochondrial calcium overload induces opening of the PTP.[38,39] In the present study, we evaluated sensitivity to calcium-induced PTP opening in a skinned myofiber preparation, thereby eliminating the potential for selection bias or experimentally induced damage associated with mitochondrial isolation procedures.[40] We found that mitochondria from *mdx* diaphragms exhibit premature PTP opening, compared with WT mice, when challenged with a calcium load. This is in keeping with the fact that damaged mitochondria, such as observed in *mdx* fibers, have a lower threshold for PTP opening. In addition, the pathological elevations of intracellular calcium and increased oxidative stress found in dystrophin-deficient muscles[4] are potent sensitizers of the PTP.[39] AICAR therapy improved the ability of *mdx* mitochondria to withstand an increased calcium load, as indicated by a normalization of the calcium exposure time needed to induce PTP opening under these conditions.

In AICAR-treated *mdx* mice, there was significant up-regulation of Ulk1, which, as noted above, has recently been identified as a direct target of AMPK that links cellular energy sensing to the process of mitophagy.[17] In addition, we observed increased expression of Bnip3, a mitochondrial BH3-only protein of the Bcl-2 family, which recruits the autophagy proteins LC3-II and Gabarap to mitochondria.[41] Bnip3 has also been strongly implicated in the process of mitophagy, and inhibition of Bnip3 impedes autophagosome formation in skeletal muscles.[42,43] Furthermore, Bnip3 is capable of stimulating mitophagy even without the requirement for mitochondrial membrane permeabilization.[44] Thus, the combined up-regulation of the mitophagy-associated proteins Ulk1 and Bnip3 in the AICAR-treated group, together with an improvement in mitochondrial PTP function, suggests that increased autophagy in treated *mdx* mice may have preferentially eliminated the mitochondrial population with a lower threshold for PTP opening.

In addition to stimulating mitophagy, AMPK activation by AICAR has the potential to induce mitochondrial biogenesis, which could also have beneficial effects on muscle function.[16] In this regard, forced expression of PGC-1-α has been shown to mitigate aging-associated muscle atrophy,[45] as well as muscle pathology in *mdx* mice.[7] The latter effect could be, at least in part, related to the fact that utrophin, a protein capable of functionally compensating for the absence of dystrophin, is expressed at higher levels in fibers with a greater oxidative capacity.[7] In the present study, however, there was no increase in utrophin protein within the diaphragms of AICAR-treated *mdx* mice. This is consistent with the absence of any detectable change in mitochondrial content (as reflected by citrate synthase) or functional indices of oxidative capacity (as determined by several complementary molecular and physiological assays, including direct measurements of fatigue resistance during repetitive muscle contractions induced by electrical stimulation). Our data are thus in keeping with prior observations that AICAR effects on mitochondrial biogenesis are minimal in muscles that are already highly oxidative,[16,46] such as the diaphragm. Accordingly, we conclude that the beneficial

effects of AICAR treatment on the *mdx* diaphragm were not the result of increased mitochondrial biogenesis or other factors specifically linked to oxidative metabolism (although it has recently been reported that this could be an additional advantage of activating AMPK in more glycolytic *mdx* muscles[25]). Furthermore, we do not exclude the possibility that AICAR exerts other biological effects beyond autophagy that could be beneficial for dystrophic muscles (eg, altered glucose uptake), nor that the relative importance of these effects may also vary among different muscles.[25]

Given that many DMD patients ultimately die of respiratory muscle failure, the most clinically relevant finding of the present study is that AICAR administration improved *mdx* diaphragm force-generating capacity. There are several ways in which the autophagic removal of damaged mitochondria could account for this finding. Although we initially postulated that eliminating damaged mitochondria would reduce oxidative stress arising from dystrophic fibers, diminished reactive oxygen species production from mitochondria (as determined by direct H_2O_2 release measurements) could not be demonstrated in the AICAR-treated group. However, damaged mitochondria are also impaired in their ability to effectively buffer elevated cytosolic calcium levels, which has been implicated in numerous aspects of dystrophic pathophysiology.[4] This can include activation of calpains and other proteolytic enzymes,[23] as well as the triggering of proinflammatory pathways regulated by NF-κB.[47] In addition, mitochondrial membrane permeabilization leads to the release of several apoptosis and muscle injury-promoting factors.[14,15] By initiating disassembly of the sarcomeric apparatus, these factors play an important role in the early phases of muscle atrophy and in depressing specific force production even when atrophy is not yet present.[48] In this regard, we observed that levels of a 14-kDa actin cleavage product previously associated with caspase-3 activation in muscle-wasting conditions[28,29] was elevated in *mdx* but not in WT mice *in vivo*, and that the presence of this cleavage product was also significantly attenuated by AICAR treatment. Our results are thus compatible with previous studies showing muscle fiber necrosis and wasting to be attenuated by interventions that inhibit or desensitize the PTP in dystrophic mice.[13,49]

In summary, treatment of *mdx* mice with the AMPK agonist AICAR significantly mitigated histological signs of pathology and improved contractile function of the diaphragm in the *mdx* mouse model of DMD. These beneficial effects were associated with induction of the autophagy program and evidence for improved mitochondrial integrity in dystrophic muscle fibers. Given the current availability of commonly used drugs (eg, metformin) that stimulate AMPK, our findings suggest that AMPK could represent a useful therapeutic target in DMD. Indeed, at a dose of metformin often prescribed for diabetes therapy (2 g/day), provided over 10 weeks, both AMPK activity and phospho-AMPK levels increased by approximately 80% over baseline levels in skeletal muscle of human subjects.[50] This is similar to the magnitude of increase in phospho-AMPK levels observed with AICAR treatment in the present study. We therefore propose that pharmacological stimulation of AMPK to enhance the autophagic removal of damaged cellular constituents, including mitochondria, is worthy of further clinical exploration as a therapy in DMD, and may also have broader applicability to other forms of skeletal muscle pathology.

Acknowledgments

We thank Johanne Bourdon and Christian Lemaire for expert technical assistance.

References

1. Koenig M, Hoffman EP, Bertelson CJ, Monaco AP, Feener C, Kunkel LM: Complete cloning of the Duchenne muscular dystrophy (DMD) cDNA and preliminary genomic organization of the DMD gene in normal and affected individuals. Cell 1987, 50:509–517
2. Tidball JG, Albrecht DE, Lokensgard BE, Spencer MJ: Apoptosis precedes necrosis of dystrophin-deficient muscle. J Cell Sci 1995, 108:2197–2204
3. Stedman HH, Sweeney HL, Shrager JB, Maguire HC, Panettieri RA, Petrof B, Narusawa M, Leferovich JM, Sladky JT, Kelly AM: The mdx mouse diaphragm reproduces the degenerative changes of Duchenne muscular dystrophy. Nature 1991, 352:536–539
4. Petrof BJ: Molecular pathophysiology of myofiber injury in deficiencies of the dystrophin-glycoprotein complex. Am J Phys Med Rehabil 2002, 81(11 Suppl):S162–S174
5. Kuznetsov AV, Winkler K, Wiedemann FR, von BP, Dietzmann K, Kunz WS: Impaired mitochondrial oxidative phosphorylation in skeletal muscle of the dystrophin-deficient mdx mouse. Mol Cell Biochem 1998, 183:87–96
6. Chen YW, Zhao P, Borup R, Hoffman EP: Expression profiling in the muscular dystrophies: identification of novel aspects of molecular pathophysiology. J Cell Biol 2000, 151:1321–1336
7. Handschin C, Kobayashi YM, Chin S, Seale P, Campbell KP, Spiegelman BM: PGC-1alpha regulates the neuromuscular junction program and ameliorates Duchenne muscular dystrophy. Genes Dev 2007, 21:770–783
8. Hardie DG: AMP-activated/SNF1 protein kinases: conserved guardians of cellular energy. Nat Rev Mol Cell Biol 2007, 8:774–785
9. Levine B, Kroemer G: Autophagy in the pathogenesis of disease. Cell 2008, 132:27–42
10. Mizushima N, Levine B, Cuervo AM, Klionsky DJ: Autophagy fights disease through cellular self-digestion. Nature 2008, 451:1069–1075
11. Youle RJ, Narendra DP: Mechanisms of mitophagy. Nat Rev Mol Cell Biol 2011, 12:9–14
12. Grumati P, Coletto L, Sabatelli P, Cescon M, Angelin A, Bertaggia E, Blaauw B, Urciuolo A, Tiepolo T, Merlini L, Maraldi NM, Bernardi P, Sandri M, Bonaldo P: Autophagy is defective in collagen VI muscular dystrophies, and its reactivation rescues myofiber degeneration. Nat Med 2010, 16:1313–1320
13. Palma E, Tiepolo T, Angelin A, Sabatelli P, Maraldi NM, Basso E, Forte MA, Bernardi P, Bonaldo P: Genetic ablation of cyclophilin D rescues mitochondrial defects and prevents muscle apoptosis in collagen VI myopathic mice. Hum Mol Genet 2009, 18:2024–2031
14. Marzetti E, Hwang JC, Lees HA, Wohlgemuth SE, Dupont-Versteegden EE, Carter CS, Bernabei R, Leeuwenburgh C: Mitochondrial death effectors: relevance to sarcopenia and disuse muscle atrophy. Biochim Biophys Acta 2010, 1800:235–244
15. Powers SK, Kavazis AN, McClung JM: Oxidative stress and disuse muscle atrophy. J Appl Physiol 2007, 102:2389–2397
16. Narkar VA, Downes M, Yu RT, Embler E, Wang YX, Banayo E, Mihaylova MM, Nelson MC, Zou Y, Juguilon H, Kang H, Shaw RJ, Evans RM: AMPK and PPARdelta agonists are exercise mimetics. Cell 2008, 134:405–415
17. Egan DF, Shackelford DB, Mihaylova MM, Gelino S, Kohnz RA, Mair W, Vasquez DS, Joshi A, Gwinn DM, Taylor R, Asara JM, Fitzpatrick J, Dillin A, Viollet B, Kundu M, Hansen M, Shaw RJ: Phosphorylation

of ULK1 (hATG1) by AMP-activated protein kinase connects energy sensing to mitophagy. Science 2011, 331:456–461
18. Demoule A, Divangahi M, Danialou G, Gvozdic D, Larkin G, Bao W, Petrof BJ: Expression and regulation of CC class chemokines in the dystrophic (mdx) diaphragm. Am J Respir Cell Mol Biol 2005, 33: 178–185
19. Chazalette D, Hnia K, Rivier F, Hugon G, Mornet D: alpha7B integrin changes in mdx mouse muscles after L-arginine administration. FEBS Lett 2005, 579:1079–1084
20. Jaber S, Petrof BJ, Jung B, Chanques G, Berthet JP, Rabuel C, Bouyabrine H, Courouble P, Koechlin-Ramonatxo C, Sebbane M, Similowski T, Scheuermann V, Mebazaa A, Capdevila X, Mornet D, Mercier J, Lacampagne A, Philips A, Matecki S: Rapidly progressive diaphragmatic weakness and injury during mechanical ventilation in humans. Am J Respir Crit Care Med 2011, 183:364–371
21. Daussin FN, Godin R, Ascah A, Deschênes S, Burelle Y: Cyclophilin-D is dispensable for atrophy and mitochondrial apoptotic signalling in denervated muscle. J Physiol 2011, 589:855–861
22. Ascah A, Khairallah M, Daussin F, Bourcier-Lucas C, Godin R, Allen BG, Petrof BJ, Des Rosiers C, Burelle Y: Stress-induced opening of the permeability transition pore in the dystrophin-deficient heart is attenuated by acute treatment with sildenafil. Am J Physiol Heart Circ Physiol 2011, 300:H144–H153
23. Bellinger AM, Reiken S, Carlson C, Mongillo M, Liu X, Rothman L, Matecki S, Lacampagne A, Marks AR: Hypernitrosylated ryanodine receptor calcium release channels are leaky in dystrophic muscle. Nat Med 2009, 15:325–330
24. Inoki K, Kim J, Guan KL: AMPK and mTOR in cellular energy homeostasis and drug targets. Annu Rev Pharmacol Toxicol 2012, 52:381–400
25. Ljubicic V, Miura P, Burt M, Boudreault L, Khogali S, Lunde JA, Renaud JM, Jasmin BJ: Chronic AMPK activation evokes the slow, oxidative myogenic program and triggers beneficial adaptations in mdx mouse skeletal muscle. Hum Mol Genet 2011, 20:3478–3493
26. Karpati G, Carpenter S, Prescott S: Small-caliber skeletal muscle fibers do not suffer necrosis in mdx mouse dystrophy. Muscle Nerve 1988, 11:795–803
27. Yang L, Lochmüller H, Luo J, Massie B, Nalbantoglu J, Karpati G, Petrof BJ: Adenovirus-mediated dystrophin minigene transfer improves muscle strength in adult dystrophic (mdx) mice. Gene Ther 1998, 5:369–379
28. Du J, Wang X, Miereles C, Bailey JL, Debigare R, Zheng B, Price SR, Mitch WE: Activation of caspase-3 is an initial step triggering accelerated muscle proteolysis in catabolic conditions. J Clin Invest 2004, 113:115–123
29. Workeneh BT, Rondon-Berrios H, Zhang L, Hu Z, Ayehu G, Ferrando A, Kopple JD, Wang H, Storer T, Fournier M, Lee SW, Du J, Mitch WE: Development of a diagnostic method for detecting increased muscle protein degradation in patients with catabolic conditions. J Am Soc Nephrol 2006, 17:3233–3239
30. Wei Y, Pattingre S, Sinha S, Bassik M, Levine B: JNK1-mediated phosphorylation of Bcl-2 regulates starvation-induced autophagy. Mol Cell 2008, 30:678–688
31. Zalckvar E, Berissi H, Mizrachy L, Idelchuk Y, Koren I, Eisenstein M, Sabanay H, Pinkas-Kramarski R, Kimchi A: DAP-kinase-mediated phosphorylation on the BH3 domain of beclin 1 promotes dissociation of beclin 1 from Bcl-XL and induction of autophagy. EMBO Rep 2009, 10:285–292
32. Lee JW, Park S, Takahashi Y, Wang HG: The association of AMPK with ULK1 regulates autophagy. PLoS One 2010, 5:e15394
33. Kim J, Kundu M, Viollet B, Guan KL: AMPK and mTOR regulate autophagy through direct phosphorylation of Ulk1. Nat Cell Biol 2011, 13:132–141
34. Eghtesad S, Jhunjhunwala S, Little SR, Clemens PR: Rapamycin ameliorates dystrophic phenotype in mdx mouse skeletal muscle. Mol Med 2011, 17:917–924
35. Sandri M: Autophagy in skeletal muscle. FEBS Lett 2010, 584:1411–1416
36. Masiero E, Agatea L, Mammucari C, Blaauw B, Loro E, Komatsu M, Metzger D, Reggiani C, Schiaffino S, Sandri M: Autophagy is required to maintain muscle mass. Cell Metab 2009, 10:507–515
37. Raben N, Hill V, Shea L, Takikita S, Baum R, Mizushima N, Ralston E, Plotz P: Suppression of autophagy in skeletal muscle uncovers the accumulation of ubiquitinated proteins and their potential role in muscle damage in Pompe disease. Hum Mol Genet 2008, 17:3897–3908
38. Gunter TE, Sheu SS: Characteristics and possible functions of mitochondrial Ca(2+) transport mechanisms. Biochim Biophys Acta 2009, 1787:1291–1308
39. Rasola A, Bernardi P: Mitochondrial permeability transition in Ca(2+)-dependent apoptosis and necrosis. Cell Calcium 2011, 50:222–233
40. Picard M, Ritchie D, Wright KJ, Romestaing C, Thomas MM, Rowan SL, Taivassalo T, Hepple RT: Mitochondrial functional impairment with aging is exaggerated in isolated mitochondria compared to permeabilized myofibers. Aging Cell 2010, 9:1032–1046
41. Novak I, Kirkin V, McEwan DG, Zhang J, Wild P, Rozenknop A, Rogov V, Löhr F, Popovic D, Occhipinti A, Reichert AS, Terzic J, Dötsch V, Ney PA, Dikic I: Nix is a selective autophagy receptor for mitochondrial clearance. EMBO Rep 2010, 11:45–51
42. Hamacher-Brady A, Brady NR, Logue SE, Sayen MR, Jinno M, Kirshenbaum LA, Gottlieb RA, Gustafsson AB: Response to myocardial ischemia/reperfusion injury involves Bnip3 and autophagy. Cell Death Differ 2007, 14:146–157
43. Mammucari C, Milan G, Romanello V, Masiero E, Rudolf R, Del PP, Burden SJ, Di LR, Sandri C, Zhao J, Goldberg AL, Schiaffino S, Sandri M: FoxO3 controls autophagy in skeletal muscle in vivo. Cell Metab 2007, 6:458–471
44. Quinsay MN, Thomas RL, Lee Y, Gustafsson AB: Bnip3-mediated mitochondrial autophagy is independent of the mitochondrial permeability transition pore. Autophagy 2010, 6:855–862
45. Wenz T, Rossi SG, Rotundo RL, Spiegelman BM, Moraes CT: Increased muscle PGC-1alpha expression protects from sarcopenia and metabolic disease during aging. Proc Natl Acad Sci USA 2009, 106:20405–20410
46. Leick L, Fentz J, Bienso RS, Knudsen JG, Jeppesen J, Kiens B, Wojtaszewski JF, Pilegaard H: PGC-1{alpha} is required for AICAR-induced expression of GLUT4 and mitochondrial proteins in mouse skeletal muscle. Am J Physiol Endocrinol Metab 2010, 299:E456–E465
47. Acharyya S, Villalta SA, Bakkar N, Bupha-Intr T, Janssen PM, Carathers M, Li ZW, Beg AA, Ghosh S, Sahenk Z, Weinstein M, Gardner KL, Rafael-Fortney JA, Karin M, Tidball JG, Baldwin AS, Guttridge DC: Interplay of IKK/NF-kappaB signaling in macrophages and myofibers promotes muscle degeneration in Duchenne muscular dystrophy. J Clin Invest 2007, 117:889–901
48. Supinski GS, Callahan LA: Caspase activation contributes to endotoxin-induced diaphragm weakness. J Appl Physiol 2006, 100:1770–1777
49. Reutenauer J, Dorchies OM, Patthey-Vuadens O, Vuagniaux G, Ruegg UT: Investigation of Debio 025, a cyclophilin inhibitor, in the dystrophic mdx mouse, a model for Duchenne muscular dystrophy. Br J Pharmacol 2008, 155:574–584
50. Musi N, Hirshman MF, Nygren J, Svanfeldt M, Bavenholm P, Rooyackers O, Zhou G, Williamson JM, Ljunqvist O, Efendic S, Moller DE, Thorell A, Goodyear LJ: Metformin increases AMP-activated protein kinase activity in skeletal muscle of subjects with type 2 diabetes. Diabetes 2002, 51:2074–2081